Xanthan and Glucomannan Mixtures: Synergistic Interactions and Gelation

Gaio Paradossi,*,† Ester Chiessi,† Alberto Barbiroli,‡ and Dimitrios Fessas‡

Department of Chemical Sciences and Technologies, University of Rome "Tor Vergata", via della Ricerca Scientifica, 00133 Rome, Italy, and INFM Section B Unità Roma Tor Vergata and Department of Food and Microbiological Sciences and Technologies, University of Milan, via Celoria 2, 20133 Milano, Italy

Received November 26, 2001; Revised Manuscript Received February 5, 2002

The synergistic interaction between xanthan and glucomannan in solution and in the gel phase has been studied by circular dichroism spectroscopy and differential scanning calorimetry. The study in solution of the polysaccharidic mixture indicates a preferred stoichiometry of the interaction corresponding to a weight fraction of xanthan around 0.55. This finding is in reasonable agreement with the differential scanning calorimetry measurements carried out on the gel phase. Models from conformational analysis based on these results were formulated in terms of 1:1 and 2:1 Konjac glucomannan/xanthan molecular assemblies. The experimental and calculation results clearly indicate the involvement of the side chains of xanthan and suggest that the ordered portions of the macromolecular complex in solution act in the gel phase as junction zones.

Introduction

Synergistic interaction between two structurally different polysaccharides can cause the formation of a physical hydrogel. Many of the works that recently appeared in the field of polysaccharidic hydrogels were addressed to the understanding of the factors governing this interaction.[1] A common feature of the polysaccharide moieties giving rise to synergic gels is their intrinsic stiffness and their different topology.[2] Another factor influencing this kind of gelation process is the charge density of one of the two polysaccharidic partners as well as the nature of the counterions.[3] These considerations show at glance the complexity of the interaction pattern governing the formation of a synergic gel. As other gelling systems they are a matter of study also for food science as they represent good texturizing agents.[1]

A class of synergic gels intensively studied is the one originating from the interaction between xanthan and locust bean gum galactomannan or Konjac glucomannan.[2−7]

Xanthan is a microbial polysaccharide with a trisaccharidic branch every other glucose of the cellulosic backbone.[8−10] Each side chain bears one carboxylic group and a varying content of pyruvyl groups ranging from some fraction to 1, depending on the breeding conditions. At room temperature, in the presence of external ionic strength, xanthan is known to be in an ordered conformation as a double-stranded wormlike chain with a persistence length of about 100 nm.[11−13] The thermal behavior of xanthan solution determined by optical activity indicates an order ↔ disorder conformational transition involving the polymer side chains. Light scattering studies of this polymer in solution revealed a more complex behavior as a halving of the molecular weight was not detected[14,15] by increasing the temperature up to 70 °C.

In an interpretation of this result, the approach to an effective equilibrium state has to be carefully considered. Once the system has reached this condition, the light scattering behavior can be explained by considering the formation in the vicinity of the transition temperature of entropy-stabilized clusters made of more than two strands held together only at some points of the chain by noncovalent bonding.[14]

Among structurally different types of galactomannans, locust bean gum can be considered a natural branched copolymer with mannose and galactose as side chains, typically in the ratio of 3.5,[16] whereas Konjac glucomannan is a $\beta(1\rightarrow4)$ linked copolymer of glucose and mannose usually in a molar ratio of 1:1.6 almost randomly distributed along the chain.[17] In the latter, some branching is also present depending on the source and seasonality with a maximum branch length of 17 sugar units.[18]

Glucomannan residues are typically acetylated to an extent ranging from 5−10%. The presence of such groups confers solubility to the polysaccharide.

Both polysaccharides have some tendency to gel depending on the temperature and concentration conditions. Xanthan forms "weak gels" above 2% (w/v) in aqueous solutions,[19,20] and glucomannan from Konjac at the same concentrations is able to form thermally stable gels in the presence of alkali.[21]

In a recent work, Annable at al.[3] have focused on the influence of counterions in determining the strength of the gel in xanthan−glucomannan mixtures. According to this

* To whom correspondence may be addressed. E-mail: paradossi@stc.uniroma2.it.

† Department of Chemical Sciences and Technologies, University of Rome "Tor Vergata" and INFM.

‡ Department of Food and Microbiological Sciences and Technologies, University of Milan.

10.1021/bm010163v CCC: $22.00
Published on Web 03/12/2002

study, counterions display a competing action against the formation of a synergic gel.

The dynamic structure factor of the gel obtained from quasi elastic laser light scattering autocorrelation function[22,23] yielded an average size and a characteristic relaxation time of the gel network[24] corresponding to about 20 nm and 300 ms, respectively. These findings are indicative of a gel architecture in the nanoscale range.

Very recently a study on the synergistic interaction between xanthan and highly galactose-branched galactomannan from mosquito seeds has inferred a defined interpolymeric association pattern involved in the gelling process.[25]

In the present work we aim to study the solution features of the macromolecular complex formed by the synergistic interaction between xanthan and glucomannan and to correlate them to the junction zones responsible of the gel formation.

Experimental Section

Materials. Glucomannan from *Amorphophallus Konjac* and xanthan gum (trade name Keltrol) from *Pseudomonas campestris* were supplied by Marine Colloids Division of FMC Corp. and Kelco International Ltd, respectively. Determination of acetyl and pyruvate content carried out by proton NMR gave a degree of substitution of 0.9 and 0.6 for acetyl and pyruvate, respectively.

Degradation of glucomannan was carried out by using cellulase (EC 3.2.1.4) from *Trichoderma viride*, Sigma, lot 38H062325.

PABA, *p*-hydroxybenzoic acid hydrazide, mannose, and blue dextran were Sigma products used without further purification.

NaCl, $NaSO_4$, buffers at pH 4.00 ± 0.02 and at 7.00 ± 0.02 at 20 °C, used for glass electrode standardization, and D-(+)-glucose were Carlo Erba products and used without further purification.

Deionized water with conductivity less than 18.2 MΩ· cm used for preparing solutions was produced with a USF Elga apparatus.

Dialysis membranes with a cut off of 12000 and 600 Da were supplied by SITC (U.K.) and by Spectrapore, respectively.

Sephacryl S-100 and Sephadex G-15 from Pharmacia Biotech were used for molecular weight fractionation of glucomannan and desalting, respectively.

Micro glass electrode from Amel was used for pH determinations.

A Jasco 7850 spectrophotometer was used for UV−vis absorption.

Methods. Xanthan Solutions. Native xanthan was degraded by sonication using a VCX 400 sonicator (Sonics and Materials Inc.) with a maximum output power of 400 W at a frequency of 20 kHz equipped with a macrotip (TI-6AL-4V). The sonication was carried out with a sequence of 1 s pulse and 0.3 s standby at approximately 80% of the maximum power. Five hundred milliliter batches of 0.6% (w/v) solution of xanthan were added with 1% (v/v) of acetone as radical scavenger and solid NaCl to a concentration of 0.1 M. Sonications were carried out in an external water/ice bath in order to avoid overheating. Following this procedure two samples of xanthan were sonicated for 40 min and for 2 h, respectively. After sonication, solutions were centrifuged at 10 000 rpm at 2 °C for 1 h with a Beckman J2-21 ultracentrifuge equipped with a J14 rotor in order to separate titanium particles from tip erosion and cell debris. Solutions were dialyzed repeatedly for 1 day against 0.03 M EDTA and then exhaustively for a week against Milli-Q grade water at 4 °C.

Table 1. Molecular Weights of the Sonicated Polysaccharides

	sonication time (min)	mol wt (g/mol)
xanthan	40	8×10^5
xanthan	120	3×10^5
KGM	60	1×10^5

Glucomannan Solutions. Konjac glucomannan, hereafter indicated as KGM, was dispersed at a concentration of 0.5 (w/v) in 0.1 M acetate buffer at pH 4.5 under vigorous mechanical stirring and autoclaved for 20 min at 120 °C.

According to the procedure described above, KGM solution was sonicated for 1 h and centrifuged. The supernatant was dialyzed for a week against Milli-Q grade water at 4 °C. NaH_3 was added as a preservative, and the resulting solution was stored at 4 °C.

The molecular weight of the sonicated polysaccharides, reported in Table 1 was determined by membrane osmometry (Osmomat 090-SA, Gonotec) using membranes with a cut off of 20000 Da.

Enzymatic Degradation of KGM. To characterize the sugar composition of KGM, an enzymatic degradation was carried out as the viscosity of the sonicated samples made impracticable the analysis by NMR ^{13}C spectroscopy. The hydrolytic activity of cellulase on the $\beta(1\rightarrow4)$ glycosidic linkages of nearest neighbor glucose units allowed a degradation of KGM polymer chains to oligosaccharides. Some $\beta(1\rightarrow4)$ mannase activity was also observed in this enzyme preparation. A typical enzymatic degradation was carried out as follows: a KGM solution in acetate buffer 0.1 M at pH 4.5 was added at 37 °C with an amount of enzyme equal to 0.1 of the polysaccharide mass. Enzyme was incubated at 37 °C for 1 h prior to the addition to the polysaccharide solution. After 20 min, degradation was stopped by adding an amount of precipitant (2-propanol). The saccharidic moiety was washed with 2-propanol and dried. ^{13}C NMR determination was carried out with a Brüker AM400 working at 100.63 MHz on 5% (w/v) solutions of degraded KGM. Chemical shifts were determined with respect to dimethyl sulfoxide. The information directly obtained from the C1 region of the degraded KGM spectra is based on the assignments available in the literature for glucomannan from cell walls of endosperm of *A. officinalis*.[26] The resonances grouped around 104 ppm and around 101.6 ppm were assigned to the nonreducing anomeric carbons of β-D-glucose residues and of the β-D-mannose residues, respectively. C1 resonances of reducing glucose and mannose units ranged from 93.4 to 97.4 ppm. On this basis it was possible to evaluate the ratio mannose/glucose of KGM, the number average degree of polymerization of the oligosaccharides

Table 2. Chemical Characteristics of KGM Oligomers[a]

	incubation time 15 min	incubation time 30 min
Man/Glc	1.7/1	1.6/1
$[DP]_n$	23	5.2
$[DP]_n$[b]		5.1
acetyl content	6.5%	6.8%

[a] Errors within 10%. [b] Determined by PABA assay.[27]

obtained after degradation, and the acetyl content. The results are reported in Table 2.

Circular Dichroism. The spectra were recorded with a JASCO J600 spectropolarimeter in the UV range 200−280 nm with quartz cells with an optical path of 0.5 and 0.1 cm. Temperature was controlled with a LAUDA M3 thermostat.

Differential Scanning Calorimetry. Volumes of stock xanthan solutions with a molecular weight of 800000 g/mol at 0.48% (w/v) and intact KGM at 0.3% (w/v), respectively, were mixed in order to yield mixtures with the desired weight ratio with a total final polysaccharide concentration of 0.34% (w/v). The gel formed after the mixing was heated to 70 °C, and 0.6 mL of solution was placed in the differential scanning calorimetry (DSC) cell.

DSC measurements were carried out with a microcalorimeter (Setaram DSC III, France) using a scan rate of 0.5 K/min. The excess heat capacity, $C_{p,exc}$, i.e., the apparent heat capacity exceeding the baseline drop across the transition (sigmoid line connecting onset and offset of the signal) was obtained as already reported in the literature.[28] Raw data were processed using homemade software.[29]

Before each measurement, a previous heating (at the same scan rate) was performed. This is a common practice when running DSC of polysaccharide systems as the first heating is characterized by a strong irreproducibility caused by initial nonequilibrium states. After the first heating, the runs were performed according to a cooling−heating−cooling cycle.

The overall melting enthalpy was obtained by integrating the excess heat capacity within the explored temperature range as already described in the literature.[29]

Molecular Modeling. All simulations were performed by a Compaq Alpha XP1000 work station. Molecular modeling calculations were carried out by the program CHARMm,[30] version c26β1.

Saccharide chains were modeled in an all-atom representation, by adopting the CHARMm carbohydrate force field with a protein-like parametrization for carboxyl, pyruvyl, and acyl groups. Xanthan uronic and pyruvyl groups were considered as uncharged, simulating a complete counterion screening. Accordingly, a unity value for dielectric constant was chosen to avoid an underestimation of the electrostatic interactions. No cutoff for nonbonded interactions was used throughout the calculations. Hydrogen bonding was treated by adjusting the atomic partial charges and van der Waals parameters for donor and acceptor atoms.[31]

The xanthan−KGM macromolecular complex was modeled by considering the interaction between a xanthan chain with 5 pentasaccharide repeating units (10 backbone sugar residues corresponding to 25 residues for the whole chain) and one or two glucomannan chains, each with 6 mannose and 4 glucose residues, randomly distributed for a M/G ratio of 1.5. To evaluate the relevance of mannose and glucose residue distribution, KGM chains with different sequences were examined without observing any effect on the topology of the models.

The corresponding Cartesian coordinates were obtained by using the CHARMm internal coordinates data. The chain conformations were modulated by the (ϕ, ψ) glycosidic dihedral angles, with ϕ = [O5−C1−O1−Cn] and ψ = [C1−O1−Cn−Cn+1] in a (1→n) glycosidic linkage (n = 2, 3, or 4).

The structures for the complex were obtained by studying the potential energy as a function of distance and orientation between the chains. The oligosaccharide structures were treated as rigid bodies and examined for association in parallel and antiparallel modes. The energetically preferred structure was then subjected to a complex conjugated minimization to a derivative value of 0.01 kcal/Å or to an iterative decrease in energy less than 0.002 kcal/mol.

In general, the limit distance for a hydrogen bond occurrence was taken equal to 3.0−3.5 Å referring to an oxygen pair.

Results and Discussion

Xanthan forms weak gels at concentrations higher than 1% (w/v) imparting non-Newtonian viscoelastic properties to the solution.[19] When this charged polysaccharide is in the presence of uncharged galactomannans or glucomannans, the tendency for gelation is enhanced. It can be expected that to some extent this interaction is a function of the distribution of galactose side chains along the (1→4)β-D-mannose backbone in the case of galactomannan[6,32,33] and of the alternating sequence of glucose and mannose on the glucomannan chains. These issues are still open to discussion as nature does not provide glucomannans with a continuous variation of composition/sequence of sugar residues. As it is often the case when dealing with physically gelling systems, in this study it is assumed that the junction zone formation, responsible for the networking of the chains, is established under appropriate conditions also in solution. Therefore we addressed our investigation in the study of the interaction both in the solution and in the gel states.

We took advantage of the presence in the xanthan side chains of a carboxylic moiety, optically active in the range 200−240 nm. In the same spectral region a low acetyl content present in the KGM backbone, around 7% according to ^{13}C NMR spectra, also contributes to the overall circular dichroic effect observed in the polysaccharidic mixture. To study the circular dichroism signal in the solution state avoiding gel formation, we used xanthan and KGM with molecular weights of 10^5 and 3×10^5 (g/mol), respectively. We focused on the dependence of the dichroic signal on the mixing ratio xanthan/KGM holding constant the total polymer concentration to 0.1%.

In the absorption region of the carboxylic moieties, due to the low content of acetyl groups, the ellipticity of KGM is about one-tenth (Figure 1, trace A) of the xanthan CD signal (Figure 1, trace B) in conditions where this polymer assumes an ordered conformation, i.e., at low pH.

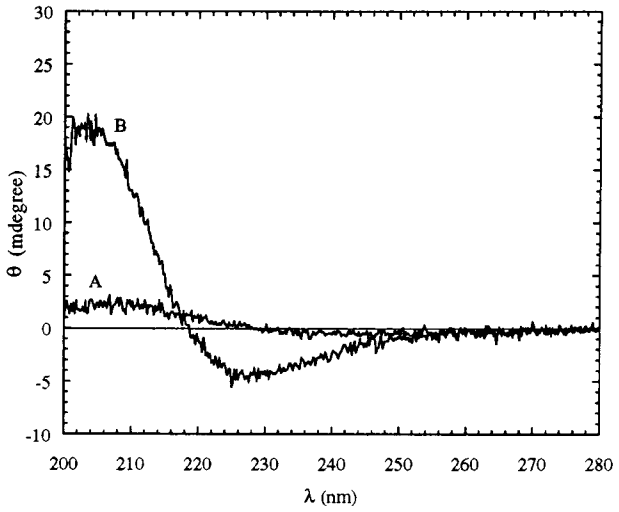

Figure 1. Circular dichroism spectra of (A) sonicated KGM solution (M_n = 100000 g/mol) and (B) sonicated xanthan solution (M_n = 300000 g/mol) at pH 4.0: polymer concentrations 0.1% (w/v); optical path 0.5 cm; 20 °C.

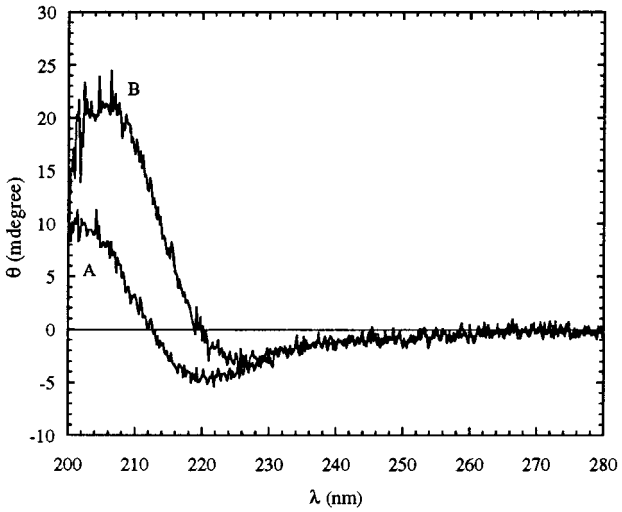

Figure 2. Circular dichroism spectra of (A) sonicated xanthan solution at pH 8.0 and concentration of 0.1% (w/v) and (B) same as A but in the presence of 0.3% (w/v) sonicated KGM: optical path 0.5 cm; 20 °C. Spectrum B was subtracted from the circular dichroism contribution of KGM.

The observed dichroic signal of dilute aqueous solutions containing KGM and xanthan was always subtracted from the contribution of KGM in order to monitor any conformational change of xanthan in the mixture. In Figure 2 the difference spectrum of a KGM/xanthan mixture at a weight ratio 3:1 at 20 °C and pH 8.0 is reported. It is noteworthy that in conditions where the xanthan chain is disordered (Figure 2, trace A), i.e., low polymer concentration and neutral pH, the interaction between xanthan and KGM causes approximately a doubling of the intensity of the dichroic band (trace B) subtracted from KGM contribution. Spectrum B shows a close similarity with the ellipticity of xanthan in ordered conformation at low pH showed in Figure 1. It was suggested that in the ordered conformation, the side chains of xanthan lye along the chain axis.[34] Taking into account that the chromophore groups of xanthan are situated in the side chains, it can be asserted that the synergic interaction involves this part of the xanthan moiety. This conclusion

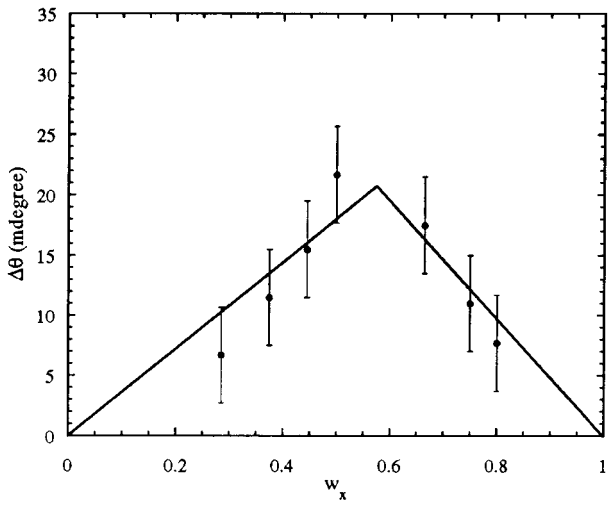

Figure 3. Ellipticity at 210 nm of xanthan/KGM solutions as a function of the weight fraction of xanthan, w_x. Contributions of the pure polymers were subtracted. Total concentration 0.3% (w/v); pH 8.0; T = 20 °C.

was also drawn by Annable et al. by means of electron paramagnetic resonance measurements using a spin label attached to xanthan side chains.[3]

To assess a stoichiometry to the complex formation, a "Job plot"[35] has been constructed on the basis of the observed ellipticities at 210 nm, θ_{obs}, corresponding to different composition of xanthan−KGM mixtures. The quantity $\Delta\theta$ reported in Figure 3 is defined as

$$\Delta\theta = \theta_{obs} - [\theta_{0,x} w_x + \theta_{0,KGM}(1 - w_x)] \qquad (1)$$

where $\theta_{0,x}$ and $\theta_{0,KGM}$ are the ellipticities of the pure polymers and w_x represents the weight fraction of xanthan.

The maximum present at a w_x value ranging between 0.5 and 0.6 indicates the mixture composition reflecting the stoichiometry of the xanthan−KGM complex. Whether this noncovalent association is effectively coupled with a conformational transition of xanthan was considered in the investigation of the temperature dependence of xanthan ellipticity. The difference spectra are reported in Figure 4 as a function of the temperature. The insert of Figure 4, showing the 210 nm ellipticity in the temperature range from 20 to 65 °C, indicates a cooperative trend probably related to the melting of an ordered structure of xanthan with a transition temperature at about 58 °C.

The thermal behavior of the gel phase was investigated by DSC to understand whether the precursor element of the gel formation is present also in the solution containing both the polysaccharide components. In this hypothesis we could identify the ordered conformation assumed by xanthan in association with KGM as the junction zones of the network responsible of the formation of a synergic gel.

Some of the DSC thermograms carried out on the aqueous mixture of xanthan/KGM at the indicated mixing ratios are shown in Figure 5. In this study intact KGM and xanthan with a molecular weight 800000 g/mol were used. For all the mixtures investigated, an almost reversible peak was observed, with a limited hysteresis characterizing the thermal cycle. The enthalpic effect normalized by the total mass of polymer is 12.1 J/g in heating and in cooling modes. At

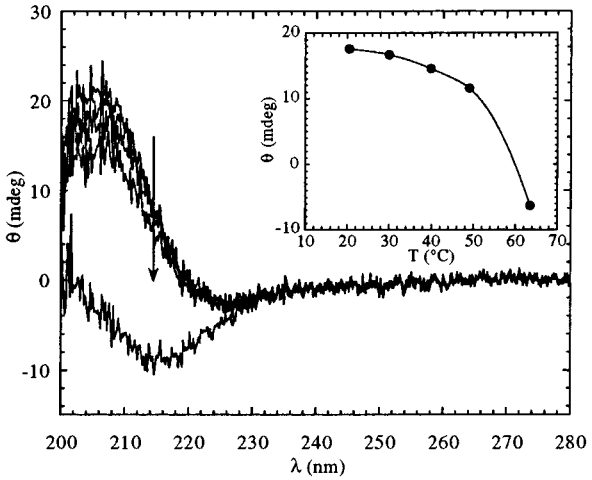

Figure 4. Circular dichroism spectra of a xanthan/KGM solution at increasing temperatures of 20, 30, 40, 49, and 63 °C, as indicated by the arrow: xanthan concentration 0.1% (w/v); xanthan/KGM weight ratio 1:3; pH 8.0; optical path 0.5 cm. Insert: Ellipticity at 210 nm of the xanthan/KGM solution as a function of the temperature.

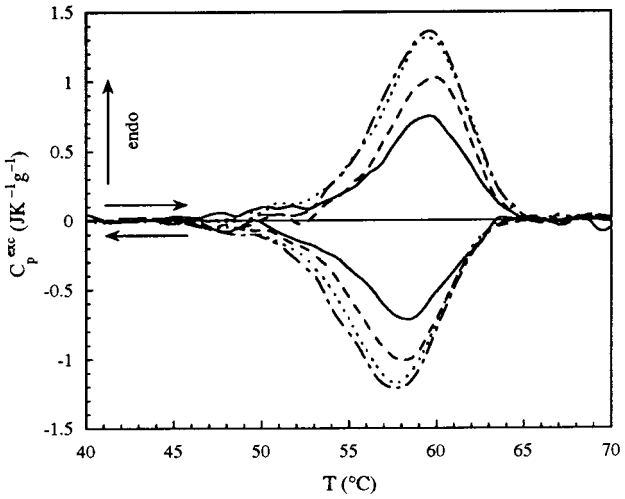

Figure 5. DSC thermograms (0.5 K/min) for xanthan/KGM mixtures, $C_{p,tot} = 0.4\%$ (w/v): weight fraction of xanthan, w_x, 0.28, 0.38, 0.44, and 0.52.

constant total polymer concentration the transition temperature was independent from the mixing ratio, indicating an enhanced invariance of the structural features of structurally well-defined regular assemblies responsible for the gel formation. In solutions containing only xanthan or KGM at a concentration of 0.48% w/v and 0.30%, respectively, it was not possible to detect any thermal effect within the range of temperatures explored. Inspection of Figure 5 shows that for increasing xanthan weight fraction the enthalpic effect increases, leveling off around $w_x = 0.55$ in agreement with the finding obtained by circular dichroism in the sol phase (Figure 3) and the results of Goycoolea et al.[5] obtained in the presence of 10 mM KCl.

Comparison of the results obtained in the sol and in the gel phases indicates the existence of a preferential weight stoichiometry, w_x, ranging between 0.5 and 0.6.

The xanthan/KGM mixtures were described by means of the "falling ball" method at a constant total polymer concentration in order to test the consistency of the gel phase as a function of the temperature and of the polysaccharide

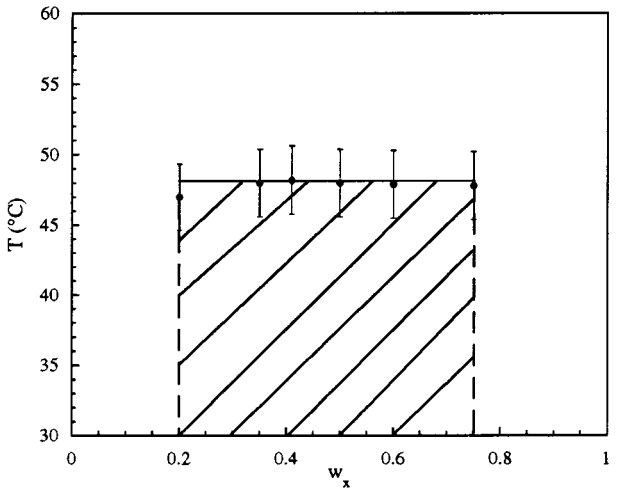

Figure 6. Sol−gel phase diagram of the xanthan/KGM mixture. Xanthan number average molecular weight is 800000 and KGM is an undegraded sample. Total concentration 0.4% (w/v).

composition and to confirm the solidlike nature of the mixtures studied by DSC. To this purpose the same conditions used for the DSC study in solution were employed. As shown in Figure 6, the gel phase is obtained in the composition range from about 0.2 to 0.8 with a constant temperature, T_{gel}.

As expected the T_{gel} obtained in this way is not quantitatively comparable with the results of DSC due to the coarse estimation of the transition temperature of this mechanically perturbative method.

The presence of the same structurally defined macromolecular complex both in gel and in sol phases led us to a modeling of the complex based on the conformational analysis.

Unfortunately at the total polymer concentration used in our determinations any detailed structural information derived from diffraction methods was unavailable.

Therefore we modeled the complex considering the stoichiometry experimentally determined as one of the requirements to be matched in working out the conformational investigation of the macromolecular assemblies although the synergic polysaccharide gel formation does not always imply the existence of a preferential composition of the mixture as is the case of xanthan/locust bean gum mixtures.[5,25]

The hypothesis of a molecular model for the description of a xanthan−KGM complex in solution was formulated considering that the glucomannan chain is characterized by a 10% branching of varying lengths. Samples of KGM with branch lengths up to 17 saccharidic residues have been reported, although usually chains with smaller degrees of branching and with much shorter branches are found. The models were formulated for two types of KGM chains, with a residue average molecular weight of 173 and of 467, corresponding to a linear chain and to a chain having 18 sugar unit branches with a degree of branching equal to 0.1, respectively.

Considering a xanthan weight fraction of 0.55 with a mass per unit length of 960 g/mol·nm and of 346 g/mol·nm for xanthan and for a linear KGM chain, respectively, a

molecular assembly of two glucomannan chains *per* chain of xanthan is obtained. Alternatively a mass per unit length of 934 g/mol·nm that accounts for the branched KGM and a xanthan weight fraction of 0.55 lead to a 1:1 glucomannan/xanthan assembly.

In formulation of the macromolecular assemblies, 2_1 and 5_1 backbone conformations were considered. X-ray diffraction patterns obtained from oriented fibers suggest a helical conformation with 5-fold symmetry for xanthan (pitch of 47.4 Å)[36,37] and a cellulose-like 2-fold helix for KGM (pitch of 10.4 Å).[38] An X-ray diffraction and modeling study on fibers of xanthan−galactomannan yielded for the complex both 2_1 and 5_1 backbone symmetry models.[39] Diffraction data on xanthan−KGM fibers[40] revealed a new structure with a helical pitch of 56 Å, suggesting an irregular arrangement of extended 2_1 chains or a 6-fold structure with a similar rise per residue found in the 5-fold helix structure of xanthan alone.[41]

On this ground, we focused on two classes of molecular models for the xanthan−KGM complex. They both consist of duplex or, alternatively, triplex oligosaccharidic chains. In one class, a pseudo 2_1 conformation was adopted for the backbone chains in a noncoaxial arrangement of cellulose-like xanthan and glucomannan helices. In a second class, a xanthan-like 5-fold helical conformation was used for the two polysaccharide moieties.

In the molecular assemblies based on the extended 2_1 backbone conformation (not shown) the polysaccharidic chains are paired together in both the 1:1 and 2:1 KGM/xanthan complex with a mean helical axes separation of about 8 Å. The xanthan moiety maintains the already reported extended pseudo-2_1 conformation[42] characterized by a backbone O5···O3 intramolecular hydrogen bond with the xanthan side facing on the same side of the helix. We must point out that this arrangement, although suggested in the modeling of xanthan/guar galactomannan interactions in fibers,[39] is quite far from the picture of the ordered xanthan conformation in solution where the side chains are placed around the helical axis. In this situation the side chain involvement to the synergic complex is marginal and does not account for the circular dichroism findings.

The 5_1 assembly is expected to be closer to the solution ordered conformation of xanthan.

Model 1:1. In Figure 7 we show the double helical arrangement of xanthan and KGM describing the complex. In analogy with the xanthan double helix, the chains of the models are in antiparallel orientation and the pseudo 5_1 helices are right-handed, with a limited perturbation with respect to the ordered double helical xanthan conformation.

In Table 3 the conformation dihedral angles are listed. The structure is stabilized by favorable van der Waals interactions and a network of intermolecular hydrogen bonds between the KGM and xanthan backbone.

Model 2:1. A satisfactory molecular packing could be obtained for a topology with two parallel glucomannan chains and xanthan in antiparallel orientation. The corresponding structure is shown in Figure 8 and the average conformation dihedral angles are given in Table 3. The saccharide backbones are in a pseudo 5-fold helix conformation with a lateral separation between helical axes of about 9.5 Å. Xanthan side chains are in an intermediate disposition between the parallel-to-backbone and the fully stretched arrangement moving away the helical symmetry to improve the intermolecular interactions. Some intramolecular hydrogen bonds are maintained, and intermolecular hydrogen bondings occur between xanthan side chain and glucomannan oxygen atoms and between oxygen atoms belonging to two KGM chains.

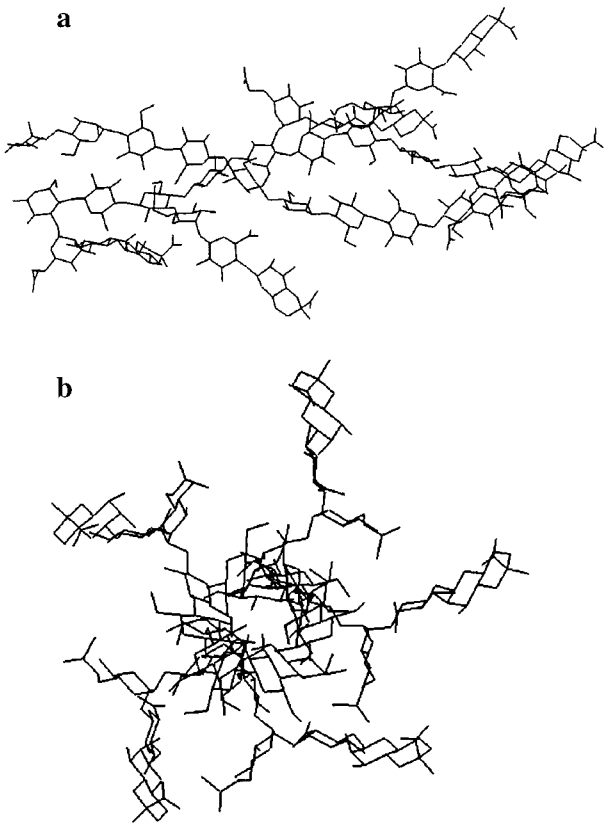

Figure 7. Molecular model of the 1:1 KGM/xanthan complex in the 5_1 topology: (a) side view; (b) view along the helix axis. Hydrogen atoms are not shown.

Table 3. Backbone Conformation Dihedral Angles[a] in Model 1:1 and Model 2:1 of KGM/Xanthan Complex

parameter	saccharide chain	model 1:1	model 2:1
ϕ^b	xanthan	-84 ± 1	-85 ± 2
ψ^b	xanthan	-104 ± 3	-102 ± 1
ϕ^c	xanthan	-72 ± 2	-75 ± 1
ψ^c	xanthan	-136 ± 4	-133 ± 1
ϕ^b	glucomannan 1	-86 ± 7	-82 ± 2
ψ^b	glucomannan 1	-100 ± 3	-102 ± 3
ϕ^c	glucomannan 1	-68 ± 4	-72 ± 2
ψ^c	glucomannan 1	-140 ± 4	-138 ± 1
ϕ^b	glucomannan 2		-82 ± 2
ψ^b	glucomannan 2		-105 ± 5
ϕ^c	glucomannan 2		-71 ± 4
ψ^c	glucomannan 2		-137 ± 4

[a] Average values. [b] First glycosidic linkage from the nonreducing end of the oligosaccharide. In the case of xanthan this linkage points toward the side chain substituted glucose residue. [c] Second glycosidic linkage from the nonreducing end of the oligosaccharide. In the case of xanthan this linkage points toward the unsubstituted glucose residue.

Concluding Remarks

This investigation has highlighted the importance of the local order in the xanthan/KGM complex in solution. The

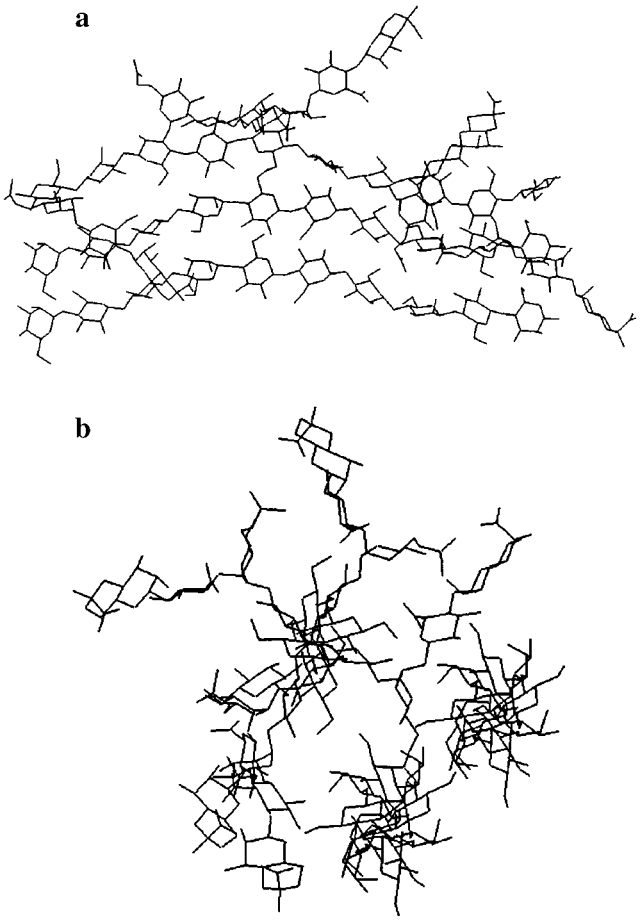

Figure 8. Molecular model of the 2:1 KGM/xanthan complex in the 5_1 topology: (a) side view; (b) view along the helix axis. Hydrogen atoms are not shown.

portions of chains organized in a ordered state seem to be the precursors of the junction zones responsible for the gel formation. The results of the circular dichroism study of the polysaccharidic mixture in solution indicate an involvement of the side chains of xanthan in association with KGM. In this respect the modeling of the junction zones according to models based on the xanthan-ordered conformation seems a more realistic picture for the ordered state within the gel network as the side chains are directionally projected toward the glucomannan moiety. The melting temperature of the ordered regions of the macromolecular complex in solution detected by circular dichroism is consistent with the corresponding temperature of melting of the gel phase. This evidence supports our hypothesis concerning the coincidence of the ordered parts of the complex and of the gel junction zones.

Finally, the ability of this saccharidic system to uptake water should be stressed, as 0.5% (w/v) of the overall polysaccharidic moiety is sufficient for obtaining firm hydrogels, confirming the potentiality of this material in fields such as food industry.

Acknowledgment. This work was supported by the MURST Fund, 9903263827-003. We acknowledge with thanks Professor A. Schiraldi for helpful discussions.

References and Notes

(1) Morris, E. R. In *Food Gels*; Harris, P., Ed.; Elsevier: London, 1990.
(2) Schorsch, C.; Garnier, C.; Doublier, J. L. *Carbohydr. Polym.* **1997**, *34*, 165−175.
(3) Annable, P.; Williams, P. A.; Nishinari, K. *Macromolecules* **1994**, *27*, 4204−4211.
(4) Ojinnaka, C.; Brownsey, G. J.; Morris, E. R.; Morris, V. J. *Carbohydr. Res.* **1998**, *305*, 101−108.
(5) Goycoolea, F. M.; Richardson, R. K.; Morris, E. R.; Gidley, M. J. *Macromolecules* **1995**, *28*, 8308−8320.
(6) Bresolin, T. M. B.; Sander P. C.; Reicher, F.; Sierakowski M. R.; Rinaudo M.; Ganter, J. L. M. S. *Carbohydr. Polym.* **1997**, *33*, 131−138.
(7) Rinaudo, M.; Milas, M.; Bresolin, T.; Ganter, J. *Macromol. Symp.* **1999**, *140*, 115−124.
(8) Pettitt, D. J. In *Food Hydrocolloids*; Gliksman, M., Ed.; CRC Press: Boca Raton, FL, 1982; Vol. 1 pp 127−149.
(9) Jansson, P. E.; Kenne, L.; Lindberg, B. *Carbohydr. Res.* **1975**, *45*, 275−282.
(10) Melton, L. D.; Mindt, L.; Rees, D. A.; Sanderson, G. R. *Carbohydr. Res.* **1976**, *46*, 245−257.
(11) Paradossi, G.; Brant, D. A. *Macromolecules* **1982**, *15*, 874−879.
(12) Schmidt, M.; Paradossi, G.; Burchard, W. *Makromol. Chem., Rapid Commun.* **1985**, *6*, 767−772.
(13) Sato, T.; Norisuye, T.; Fujita, H. *Polym. J.* **1984**, *16*, 341−350.
(14) Haccke, L. S.; Washington, G. E.; Brant, D. A. *Macromolecules* **1987**, *20*, 2179−2187.
(15) Liu, W.; Norisuye, T. *Biopolymes* **1988**, *27*, 1641−1654.
(16) Dea, I. C. M.; Morrison, A. *Adv. Carbohydr. Chem. Biochem.* **1975**, *31*, 241−250.
(17) Nishinari, K.; Williams, P. A.; Phillips, G. O. *Food Hydrocolloids* **1992**, *6*, 199−222.
(18) Maeda, M.; Shinahara, H.; Sugiyama, N. *Agric. Biol. Chem.* **1980**, *44*, 245−252.
(19) Oviatt, H. W.; Brant, D. A. *Int. J. Biol. Macromol.* **1993**, *15*, 3−10.
(20) Rodd, A. B.; Dunstan, D. E.; Boger, D. V. *Carbohydr. Polym.* **2000**, *42*, 159−174.
(21) Zhang, H.; Yoshimura, M.; Nishinari, K.; Williams M. A.; Foster, T. J.; Norton, I. T. *Biopolymers* **2001**, *59*, 38−50.
(22) Pusey, P. N.; van Megen, W. *Physica A* **1989**, *157*, 705−741.
(23) Xue, J. Z.; Pine, D. J.; Milner, S. T.; Wu, X. I.; Chaikin, P. M. *Phys. Rev. A* **1992**, *46*, 6550−6563.
(24) Bordi, F.; Paradossi, G.; Rinaldi, C.; Rutzika, B. *Physica A* **2002**, *304*, 119−128.
(25) Goycoolea, F. M.; Milas, M.; Rinaudo, M. *Int. J. Biol. Macromol.* **2001**, *29*, 181−192.
(26) Goldberg, R.; Gillou, L.; Prat, R.; Herve du Penhoat, C.; Michon, V. *Carbohydr. Res.* **1991**, *210*, 263−276.
(27) Lever, M. *Anal. Biochem.* **1972**, *47*, 273−279.
(28) Freire, E.; Biltonen, R. L. *Biopolymers* **1978**, *17*, 463−479.
(29) Barone, G.; Del Vecchio, P.; Fessas, D.; Giancola, C.; Graziano, G. *J. Therm. Anal.* **1992**, *38*, 2779−2790.
(30) Brooks, B. R.; Bruccolieri, R. E.; Olafson, B. D.; States, D. J.; Swaminathan, S.; Karplus, M. *J. Comput. Chem.* **1983**, *4*, 187−217.
(31) Brady, J. W.; Schmidt, R. K. *J. Phys. Chem.* **1993**, *97*, 958−966.
(32) Bresolin, T. M. B.; Milas, M.; Rinaudo, M.; Reicher, F.; Ganter, J. L. M. S. *Int. J. Biol. Macromol.* **1999**, *26*, 225−231.
(33) Cheetam, N. W. H.; Mashimba, E. N. M. *Carbohydr. Polym.* **1988**, *9*, 195−201.
(34) Gamini, A.; de Blijser, J.; Leyte, J. C. *Carbohydr. Res.* **1991**, *220*, 33−47.
(35) Cantor, C. R.; Schimmel, P. R. *Biophysical Chemistry*; Freeman Co.: San Francisco, CA, 1980; Part II; Chapter 22, pp 1135−1138.
(36) Moorhouse, R.; Walkinshaw, M. D.; Arnott, S. *ACS Symp. Ser.* **1977**, *No. 45*, 90−102.
(37) Okuyama, K.; Arnott, S.; Moorhouse, R.; Walkinshaw, M. D.; Atkins, E. D. T.; Wolf-Ullish, C. *ACS Symp. Ser.* **1980**, *No. 141*, 411−427.
(38) Yui, T.; Ogawa, K.; Sarko, A. *Carbohydr. Res.* **1992**, *229*, 41−55.
(39) Chandrasekaran, R.; Radha, A. *Carbohydr. Polym.* **1997**, *32*, 201−208.
(40) Brownsey, G. J.; Cairns, P.; Miles, M.; Morris, V. J. *J. Carbohydr. Res.* **1988**, *176*, 329−334.
(41) Morris, V. J. In *Gums and Stabilizers for the Food Industry 6*; Phillips, G. O., Williams, P. A., Wedlock, D. J., Eds.; IRL Press: Oxford, 1992; pp 161−171.
(42) Millane, R. P.; Wang, B. *Carbohydr. Polym.* **1990**, *13*, 57−68.

BM010163V